

### 3D color CT and MRI of muscle, bone and brain

Eur J Trans Myol - Basic Appl Myol 2014; 24 (1): 55-62

## CT and MRI assessment and characterization using segmentation and 3D modeling techniques: applications to muscle, bone and brain

(1,2) Paolo Gargiulo, (1,2) Thordur Helgason, (1,3) Ceon Ramon, (4,5) Halldór Jónsson jr, (6) Ugo Carraro

(1) Institute of Biomedical and Neural Engineering (BNE), Reykjavik University, Iceland; (2) Research Department, Landspítali University Hospital, Iceland; (3) Department of Electrical Engineering, University of Washington, United States; (4) Orthopedic Clinic, Landspítali Hospital, Iceland; (5) Medical Faculty, Iceland University; (6) CIR-Myo, Translational Myology Lab, Department of Biomedical Sciences, University of Padova, Italy

### Abstract

This paper reviews the novel use of CT and MRI data and image processing tools to segment and reconstruct tissue images in 3D to determine characteristics of muscle, bone and brain. This to study and simulate the structural changes occurring in healthy and pathological conditions as well as in response to clinical treatments. Here we report the application of this methodology to evaluate and quantify: 1. progression of atrophy in human muscle subsequent to permanent lower motor neuron (LMN) denervation, 2. muscle recovery as induced by functional electrical stimulation (FES), 3. bone quality in patients undergoing total hip replacement and 4. to model the electrical activity of the brain.

*Study 1:* CT data and segmentation techniques were used to quantify changes in muscle density and composition by associating the Hounsfield unit values of muscle, adipose and fibrous connective tissue with different colors. This method was employed to monitor patients who have permanent muscle LMN denervation in the lower extremities under two different conditions: permanent LMN denervated not electrically stimulated and stimulated. *Study 2:* CT data and segmentation techniques were employed, however, in this work we assessed bone and muscle conditions in the pre-operative CT scans of patients scheduled to undergo total hip replacement. In this work, the overall anatomical structure, the bone mineral density (BMD) and compactness of quadriceps muscles and proximal femoral was computed to provide a more complete view for surgeons when deciding which implant technology to use. Further, a Finite element analysis provided a map of the strains around the proximal femur socket when solicited by typical stresses caused by an implant press fitting. *Study 3* describes a method to model the electrical behavior of human brain using segmented MR images. The aim of the work is to use these models to predict the electrical activity of the human brain under normal and pathological conditions by developing detailed 3D representations of major tissue surfaces within the head, with over 12 different tissues segmented. In addition, computational tools in Matlab were developed for calculating normal vectors on the brain surface and for associating this information with the equivalent electrical dipole sources as an input into the model.

**Key Words:** Medical modelling, Image processing, denervated muscle, brain, hip prosthesis, fracture risk

*Eur J Trans Myol - Basic Appl Myol 2014; 24 (1): 55-62*

The use of bioimages in diagnostics, treatment planning and clinical follow up is becoming more and more vital to the quality of patient treatment and outcome. In this context, technological development plays the main role with medical imaging devices being among the main investments in healthcare. The current CT and MRI devices are able to display and reconstruct in three-dimensions (3D) anatomical

details that only few years ago were unimaginable. Further, the use of high quality medical images creates new possibilities and potential in areas like modeling, simulation and analysis of the human body and its behavior. These tools are particularly important in situations where it is either: 1. too risky to perform an invasive procedure; 2. too costly for in vivo experiments; 3. impossible to address the situation

### 3D color CT and MRI of muscle, bone and brain

Eur J Trans Myol - Basic Appl Myol 2014; 24 (1): 55-62

otherwise for ethical reasons or 4. simply because the imaging can provide information otherwise impossible to obtain. However, the use of bioimages to model biomechanical or bioelectrical systems may be seriously complex because of the large number of potential variables. Indeed, a system may have such a large number of parameters that they cannot all be identified and considered. Therefore, the modeling approach, especially in biological systems, is designed according to established criteria and objectives and is usually constrained to accurately consider or describe only certain characteristics while approximating or ignoring others. In summary, today bioimages are being used in both traditional and non-traditional ways to study biological systems with the following aims: 1. to describe and simulate mechanical and/or electrical behavior of certain anatomical systems; 2. to model and analyze normal and pathological conditions; 3. to study tissue properties or to correlate different tissue characteristics; and 4. to create rapid prototype models (automatic manufacturing of physical items directly from 3D computer data) that can support surgical planning. The common denominator for these applications is the use and processing of medical images. This process involves capturing human anatomy images by scanning the patients with clinical modalities such CT and MRI devices, and the use of special image processing tools which allow for image segmentation and 3D reconstruction. Future challenges

are offered by the increased use of  $\mu$ CT technologies to study osteogenesis within biological scaffolds and bone or in soft tissues to quantify muscle quality. Also in these areas of research the use of image processing tools and segmentation techniques to analyze microstructures is becoming very important quickly. This work reviews the use of this process in three different research studies in which the authors have been involved.

#### Monitoring trophism decay of LMN denervated muscle or restoration by h-b FES compliance

Loss of muscle mass occurs with many pathological conditions and is linked to increased patient disability, morbidity and mortality,<sup>1,2</sup> thus, it is important to discover how to determine muscle degeneration. Empirical clinical observations,<sup>3</sup> revealed that lower motor neuron (LMN) denervated-degenerated muscle can recover by a specific strategy of home-based daily functional electrical stimulation (h-b FES) therapy. Based on pioneering observations the European funded project RISE was founded in 2001 with the aim to establish the biological basis for clinical rehabilitation treatment, and technological support,<sup>4</sup> for patients who have permanent muscle LMN denervation of the legs. The project encompassed a clinical trial with over 25 volunteer patients and additional animal experiments to study the muscle restoration process by combining physiological, histological, immunohistochemical,

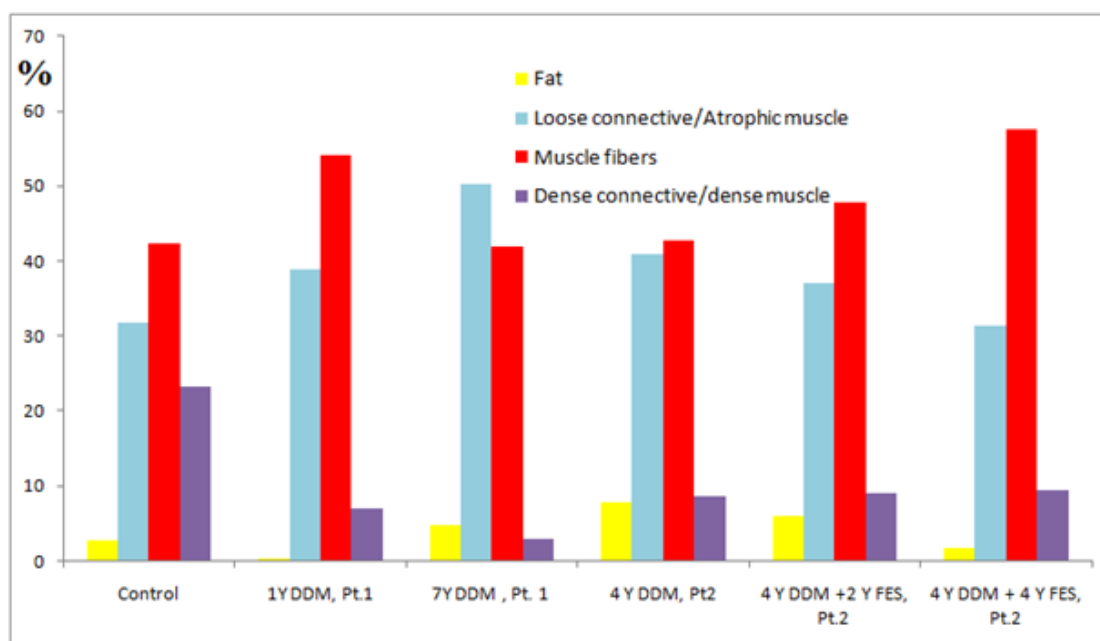


Figure 1. Histogram showing the tissue composition in denervated, degenerated muscle (DDM) rectus femoris under different physiological conditions: healthy (control), short term denervated (subject 1, 1 year after spinal cord injury (SCI)), long term denervated poorly compliant to h-b FES treatment (subject 1, 7 years after SCI) and long term denervated compliant treated for 4 years h-b FES treatment (subject 2, 8 years after SCI).

### 3D color CT and MRI of muscle, bone and brain

Eur J Trans Myol - Basic Appl Myol 2014; 24 (1): 55-62

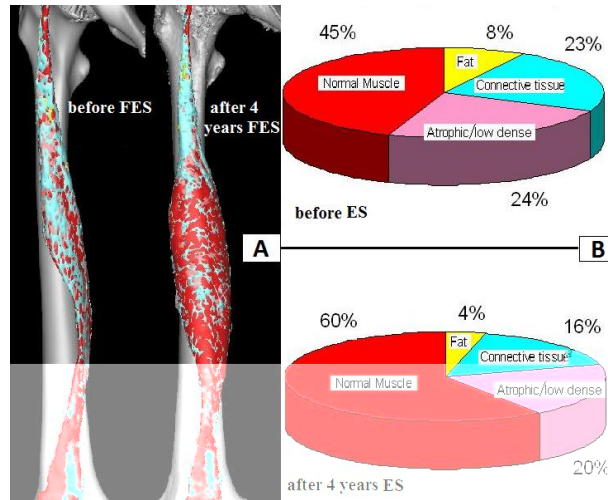


Figure 2. A, 3D color models of RF of patient 2, before and after 4 years of h-b FES treatment; B Pie charts show the muscle composition before and after 4 years of h-b FES.

electron microscopy analyses with anthropometric techniques.<sup>5-13</sup> Many of the tissue analyses employed to study structural changes occurring in LMN denervated muscle (both after long-term LMN denervation and during electrical stimulation trainings) were performed with biopsies, i.e. only a few milligrams of muscle could be analyzed.<sup>5-8</sup> Complementary imaging techniques, such as CT scan, were also employed in order to assess and validate histological information and to study macroscopic changes. The value of the imaging methods was demonstrated by studying the effect of electrical stimulation trainings on the entire muscle volume.<sup>14,15</sup> The main novelty introduced in

this work is the morphological analysis of the whole quadriceps femoris in different pathological conditions and the quantification of the tissue composition within the muscle volume. The distribution of Hounsfield unit (HU) values resulting from the 3D structural analysis of rectus femoris is depicted in the histogram in figure 1.<sup>16</sup> In this histogram, we quantify different tissues within the muscle volume by using the following thresholds: Fat [-200, -6] HU, loose connective tissue [-5, 40] HU (in this interval water and low dense muscle fibers are also displayed), muscle fibers [41, 80] HU, and dense connective tissue [81, 200] HU (in this interval dense muscle fiber are also displayed).

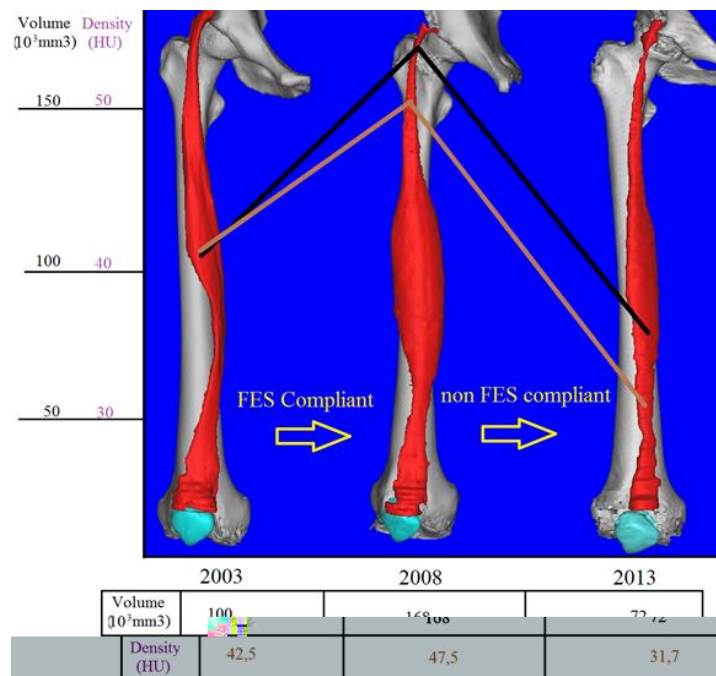


Figure 3. Increase and decline of muscle volume and density depending upon compliance to h-b FES during 10 years monitoring

### 3D color CT and MRI of muscle, bone and brain

Eur J Trans Myol - Basic Appl Myol 2014; 24 (1): 55-62

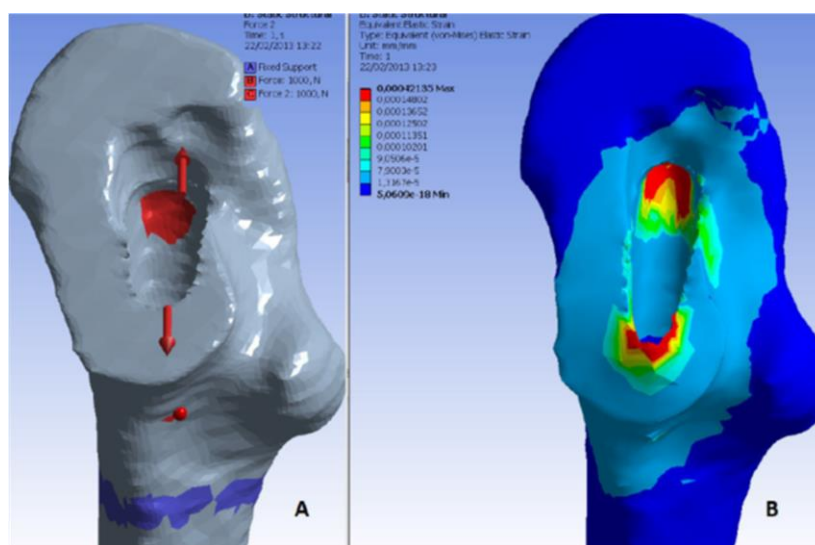


Figure 4. Uncemented simulation. A, Applied force at the proximal femur socket . B, Von Mises strain distribution.

Figure 1 shows that the loss of tissue density is mainly due to the loss of dense connective tissue after SCI. On the other hand, the FES treatment allows restoration of muscle fiber (increasing from 42% to 58% after 4 years FES) and sensible decrease of low dense muscle fibers-loose connective and fat (decreasing on average from 41% to 31% and from 8% to 2%, respectively).

To better visualize the effects induced with electrical stimulation trainings on denervated muscle volume with 3D, the HU thresholds are slightly modified and the tissues renamed in the following way: Normal muscle [40, 200] HU, atrophic/low dense muscle [20, 40] HU, connective tissue [-5, 20] HU and Fat [-200, -6] HU.

Figure 2 presents the results of Patient 2, who started h-bFES 3 years after SCI and showed a dramatic increase in muscle volume and density during the compliant period of home based functional electrical stimulation, from 2006 to 2009. In 2013, we analysed the muscle conditions for this patient once again to complete the 10 year SCI follow up. The results are displayed in figure 3 that demonstrates quite well that the cycle of growth and decline is the result of FES compliance or non compliance. After 4 years without FES, the decline of volume and density is trivial, with values falling below the 2003 starting point.

The 3D modeling technique shows very well the morphological changes which occurred within the rectus femoris (RF) muscle during this time period of lack of h-b FES.

The reversibility of the effect of training is a strong evidence that the recovery was not due to reinnervation, since disused innervated/reinnervated muscles never undergo such a tremendous loss of muscle mass.<sup>13</sup>

### Bone Mineral Density, fracture risk and muscle density assessment by 3D CT as support for decision making for patients undergoing total hip arthroplasty

Total hip arthroplasty (THA) is performed with or without the use of bone cement. The benefit of the cemented procedure is a faster achievement of implant stability compared to an uncemented procedure where the primary implant stability is secured by geometrical interlocking, press fit forces and friction between bone and implant, whilst the secondary stability is additionally secured by bone ingrowth into the surface texture of the femoral component. In the first years post-operatively, uncemented stems are more frequently in need of revision (prosthetic re-implant) than cemented stems due to periprosthetic fracture. Managing these fractures may create a real challenge for surgeons because of the poor quality of the surrounding bone.<sup>17, 18</sup> On the other hand, the revision surgery for uncemented implants has a higher success rate and generally results in fewer complications than revision surgeries for cemented implants.<sup>19-22</sup> The drawback of cemented procedures is also related to the risk of cement cracking as a result of fatigue. Overall, however, the patients survival rate of uncemented THA is still slightly inferior to that of cemented THA according to the Swedish Hip Registry.<sup>23</sup>

At our clinical center in Reikjavik, orthopedic surgeons chose between the cemented and uncemented THA procedures based upon age, sex and general health conditions, however, quantitative preoperative measurements of bone quality are not yet included in current clinical guidelines. We believe that bone and muscle quality are crucial parameters upon which orthopedic surgeons should also base the decision between cemented and cementless THA. Therefore

### 3D color CT and MRI of muscle, bone and brain

Eur J Trans Myol - Basic Appl Myol 2014; 24 (1): 55-62

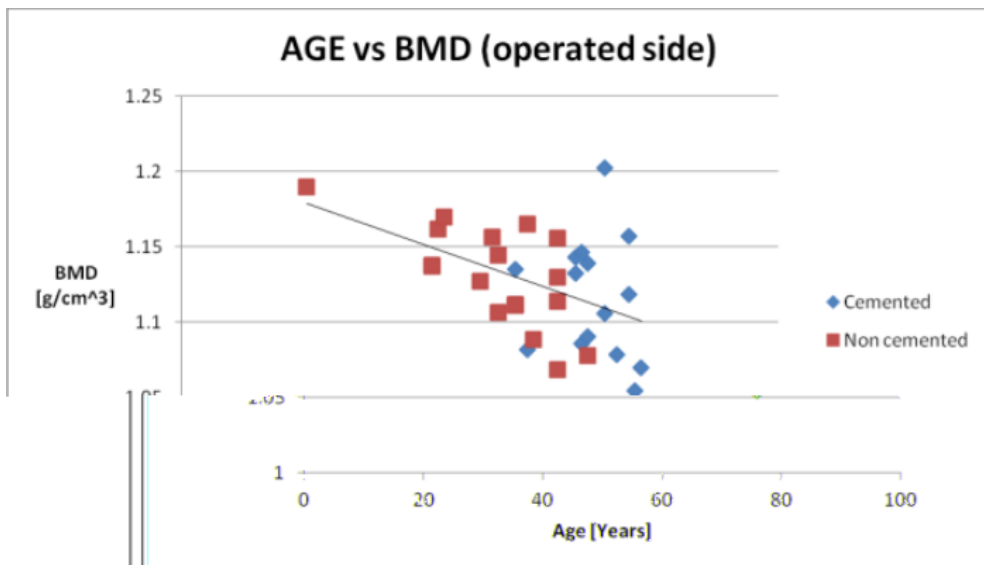


Figure 5. Bone Mineral Density [ $\text{g}/\text{cm}^3$ ] sorted by implant technique and ordered by patient age.

based upon medical image processing and finite element methods, we have been analysing Bone Mineral Density (BMD), muscle density and the fracture risk index (FRI) of patients before surgery. Thirty-six volunteer patients (20 females and 16 males) were enrolled in the clinical trial; 18 received a cemented- and 18 received an uncemented implant. The implant type to be used was determined according to the surgeons evaluation based mostly upon patient age, gender and general clinical conditions. All patients were first time THA surgeries. The average age at the moment of surgery was 56 for the males and 62 for the females; the youngest patient was 22 and the oldest was 77 years old. Patients were subjected to CT-scan (64 CT Philip Brilliance) before and immediately after surgery and again at 52 weeks post-surgery. The scanning region started from the iliac crest bone and

ended at the middle of the femur; slice thickness is 1mm, slice increment is 0.5mm. Using the segmentation methods described by Gargiulo et al. (2012),<sup>17</sup> the proximal femur and a partition of the quadriceps muscle were isolated. The proximal femur was further analysed with Finite Element Analysis software and the mechanical conditions of an uncemented prosthesis were simulated in order to estimate the fracture risk index according to the methodology described by Gargiulo et al. (2013),<sup>24</sup> Figure 4 shows the simulation scenarios with applied force, fixed support and the strain distribution. The preoperative BMD values calculated on the proximal femur (affected side) for all of the patients participating in the study are displayed in figure 5.<sup>25</sup> From the same data set, figure 6 shows rectus femoris muscle density (affected side) for all the patients

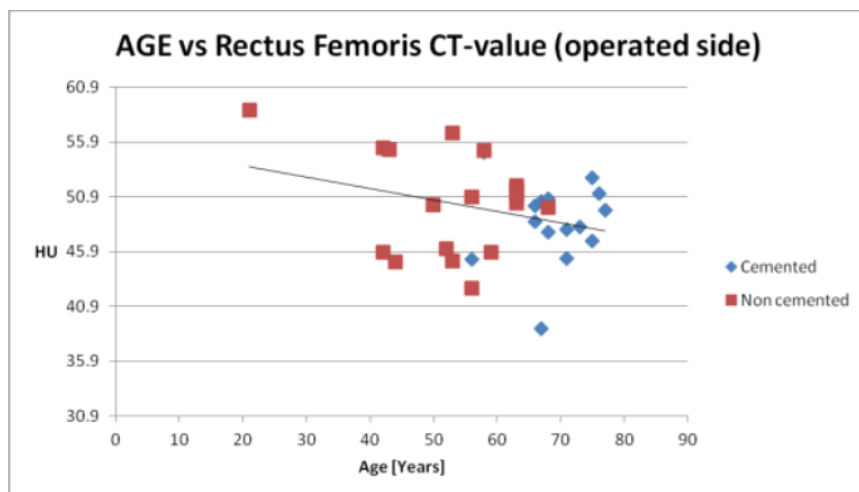


Figure 6: Rectus femoris muscle density [HU] sorted by implant technique and ordered by patient age.

### 3D color CT and MRI of muscle, bone and brain

Eur J Trans Myol - Basic Appl Myol 2014; 24 (1): 55-62

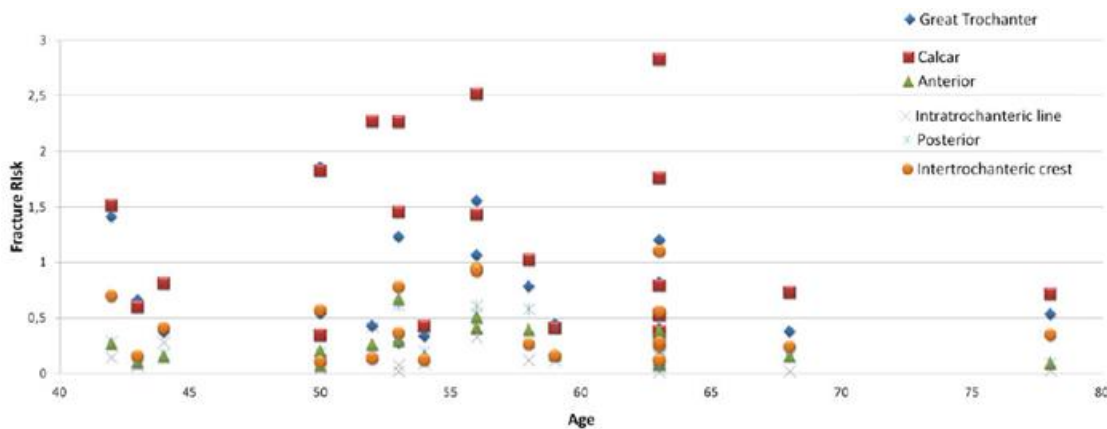


Figure 7. Fracture risk indexes calculated on different anatomical regions around the proximal femur socket from patient undergoing uncemented hip prosthesis.

participating in the study. Finally figure 7 shows the fracture risk index calculated on different anatomical regions around the proximal femur for all patients.

These results show that gender, age and general clinical condition alone aren't sufficient to provide optimal decision-making data for the implant technology employed. The results support the observation/theory that bone and muscle density, as major predictors of intraoperative and post surgical fractures, are not solely age and gender related (i.e., there is a significant overlap concerning bone/muscle density and age groups).

In conclusion, despite the fact that our Finite Element simulation is still to be improved and that the index of fracture is an underestimation of the real risk posed, the method described is a promising tool to optimize an important clinical process.

#### Segmentation of the head MRI data for modelling electrical activity of brain

In this last study, we describe a method, using segmented MR images, developed to model the electrical behaviour of human brain. The goal is to use

these models to predict the electrical activity of human brain under normal and pathological conditions. The relationship between neuronal sources and the recorded scalp Electroencephalographs (EEG's) relies on different coupled non-linear physical mechanisms.<sup>26</sup> The electrical effects of these mechanisms then distribute from their sources through inhomogeneous media with various electrical properties. Forward EEG modelling is a discipline which uses numerical techniques such as finite element modelling (FEM) to study the relationship between electrical sources in the brain and the resulting electrical potentials at the scalp.<sup>27</sup> Sources in the form of current dipoles are placed in the brain and then the FEM equations are solved for the resulting potential at the scalp. For accurate forward EEG modelling, detailed segmentation of tissues is needed, especially between the electrical source and scalp. In former studies, the model complexity, or the number of tissue types, has been shown to affect the results.<sup>28</sup> These have emphasized the role of accurate segmentation of the cerebrospinal fluid (CSF) and bone.<sup>29</sup> A detailed 3D

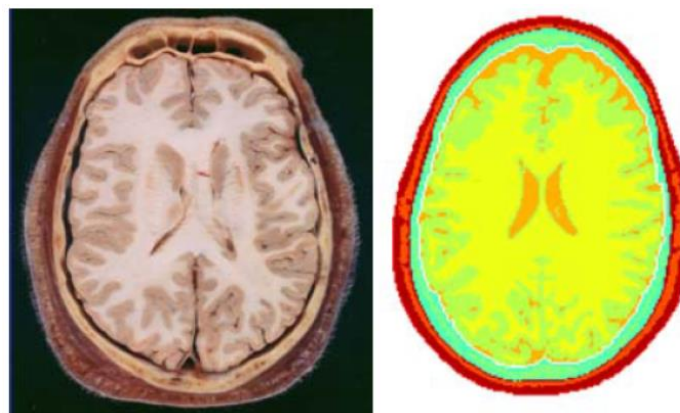


Figure 8. Segmentation results showing different tissue surfaces (Right) and the corresponding anatomical reference (Left). The head tissues are represented by different colors.

### **3D color CT and MRI of muscle, bone and brain**

Eur J Trans Myol - Basic Appl Myol 2014; 24 (1): 55-62

presentation of major tissues within the head was developed including: white and gray matter, cerebellum, CSF, cortical and trabecular bone, dura layer, skin, eyes and eye crystalline, etc.

Some of these tissues have a distinguished threshold while others are displayed within the same gray value interval. In these cases, special segmentation techniques and manual editing are employed to isolate single tissues from the surroundings. The results are shown in figure 8. A FEM model was constructed from segmented data. The voxel resolution was  $1 \times 1 \times 1$  mm. The electrical conductivities of various tissues were

### 3D color CT and MRI of muscle, bone and brain

Eur J Trans Myol - Basic Appl Myol 2014; 24 (1): 55-62

10. Squecco R, Carraro U, Kern H, et al. A subpopulation of rat muscle fibers maintains an assessable excitation-contraction coupling mechanism after long-standing denervation despite lost contractility. *J Neuropathol Exp Neurol* 2009;68:1256-68.
11. Kern H, Carraro U, Adami N, et al. One year of home-based daily FES in complete lower motor neuron paraplegia: recovery of tetanic contractility drives the structural improvements of denervated muscle. *Neurol Res* 2010;32:5-12.
12. Kern H, Carraro U, Adami N, et al. Home-based functional electrical stimulation rescues permanently denervated muscles in paraplegic patients with complete lower motor neuron lesion. *Neurorehabil Neural Repair* 2010;24:709-21.
13. Kern H, Hofer C, Mödlin M, et al. Stable muscle atrophy in long-term paraplegics with complete upper motor neuron lesion from 3-to 20-year SCI. *Spinal Cord* 2007;46:293-304.
14. Helgason T, Gargiulo P, Jóhannesdóttir F, et al. Monitoring muscle growth and tissue changes induced by electrical stimulation of denervated degenerated muscles with CT and stereolithographic 3D modeling. *Artif Organs* 2005;29:440-3.
15. Gargiulo P, Vatnsdal B, Ingvarsson P, et al. Quantitative color three-dimensional computer tomography imaging of human long-term denervated muscle. *Artif Organs* 2008;32:609-13.
16. Gargiulo P, Jens Reynisson P, Helgason, et al. Muscle, tendons, and bone: structural changes during denervation and FES treatment. *Neurol Res* 2011;33:750-8.
17. Gargiulo P, Carraro U, Mandl T, et al. Anthropometry of human muscle using segmentation techniques and 3D modelling: applications to lower motor neuron denervated muscle in Spinal Cord Injury. In *Handbook of Anthropometry*, Springer, New York, 2012 pp. 323-54.
18. Venesmaa PK, Kroger HPJ, Miettinen HJA, et al. Monitoring of periprosthetic BMD after uncemented total hip arthroplasty with Dual-Energy X-Ray Absorptiometry — a 3-year follow-up study. *J Bone Miner Res* 2001;16:1056-61. doi: 10.1359/jbmr.2001.16.6.105.
19. Engh CA, Glassman AH, Griffin WL, Mayer JG. Results of cementless revision for failed cemented total hip arthroplasty. *Clin Orthop* 1988;235:91-110.
20. Engelbrecht DJ, Weber FA, MB Sweet, I Jakim Long-term results of revision total hip arthroplasty *Bone Joint Surg Br* 1990; 72:41-5.
21. JM Lawrence, CA Engh, GE Macalino, GR Lauro Outcome of revision hip arthroplasty done without cement *J Bone Joint Surg Am* 1994; 76:965-73.
22. JR Moreland, ML Bernstein. Femoral revision hip arthroplasty with uncemented, porous-coated stems *Clin Orthop* 1995;319:141.
23. Hailer NP, Garellick G, Karrholm J. Uncemented and cemented primary total hip arthroplasty in the Swedish Hip Arthroplasty Register. *Acta Orthopaedica* 2010;81:34-41.
24. Gargiulo P, Pétursson T, Magnússon B, et al. Assessment of Total Hip Arthroplasty by Means of Computed Tomography 3D Models and Fracture Risk Evaluation. *Artif Organs* 2013;37:567-73. doi: 10.1111/aor.12033. Epub 2013 Apr 2.
25. Pétursson T, Magnússon B, Helgason B, et al. Bone and muscle assessment in patients undergoing total hip arthroplasty using HU based analysis. *Eur J Trans Myol-Basic Appl Myol* 2012;22:147-52.
26. Abraham K. and Marsan C.A. Patterns of cortical discharges and their relation to routine scalp electroencephalography. *Electroenceph. clin. neurophysiol* 1958;10:447-61.
27. Hallez, H., Vanrumste, B., Grech, R., et al. Review on solving the forward problem in EEG source analysis. *J Neuroeng Rehabil* 2007;4:46.
28. Ramon C, Schimpf PH, Haueisen J. Influence of head models on EEG simulations and inverse source localizations. *Biomed Eng Online* 2006;5:10.
29. Ramon C, Schimpf PH, Haueisen, J, et al. Role of soft bone, CSF and gray matter in EEG simulations. *Biomed Eng Online* 2004;16:245-8
30. Schimpf PH, Haueisen J, Ramon C, Nowak H. Realistic computer modeling of electric and magnetic fields of human head and torso. *Parallel Computing* 1998;24:1433-60.
31. Friðgeirsson, EA, Gargiulo P, Ramon C, Haueisen J. 3D segmented model of head for modelling electrical activity of brain. *Eur J Trans Myol-Basic Appl Myol* 2012;22:57-60.